NeuroImage 221 (2020) 117146

Contents lists available at ScienceDirect

NeuroImage

journal homepage: www.elsevier.com/locate/neuroimage

Intraparietal sulcus maintains working memory representations of somatosensory categories in an adaptive, context-dependent manner

Lisa Alexandria Velenosi [a,*], Yuan-Hao Wu [a,b,c], Timo Torsten Schmidt [a], Felix Blankenburg [a,b]

[a] Neurocomputation and Neuroimaging Unit, Freie Universität Berlin, Habelschwerdter Allee 45, Berlin, 14195, Germany
[b] Berlin School of Mind and Brain, Humboldt-Universität zu Berlin, Luisenstraße 56, Berlin, 10117, Germany
[c] NYU Grossman School of Medicine, New York University, 550 First Avenue, New York, 10016, USA

ARTICLE INFO

Keywords:
Working memory
Somatosensory
Adaptive coding
Categorization
Multivariate
fMRI

ABSTRACT

Working memory (WM) representations are generally known to be influenced by task demands, but it is not clear whether this extends to the somatosensory domain. One way to investigate the influence of task demands is with categorization paradigms, wherein either a single stimulus or an associated category is maintained in WM. In the somatosensory modality, category representations have been identified in the premotor cortex (PMC) and the intraparietal sulcus (IPS). In this study we used multivariate-pattern-analysis with human fMRI data to investigate whether the WM representations in the PMC, IPS or other regions are influenced by changing task demands. We ensured the task-dependent, categorical WM information was decorrelated from stimulus features by (1) teaching participants arbitrary, non-rule based stimulus groupings and (2) contrasting identical pairs of stimuli across experimental conditions, where either a single stimulus or the associated group was maintained in WM. Importantly, we also decoupled the decision and motor output from the WM representations. With these experimental manipulations, we were able to pinpoint stimulus-specific WM information to the left frontal and parietal cortices and context-dependent, group-specific WM information to the left IPS. By showing that grouped stimuli are represented more similarly in the Group condition than in the Stimulus condition, free from stimulus and motor output confounds, we provide novel evidence for the adaptive nature of somatosensory WM representations in the IPS with changing task-demands.

1. Introduction

Working memory (WM) is the ability to maintain and manipulate representations of stimuli which are no longer being perceived (Baddeley and Hitch, 1974) and underlies fundamental human behaviours and abilities (Logie and Cowan, 2015). As a result, identifying the neural correlates of WM is a major focus of scientific interest. Presently, a large body of evidence suggests that the localization of WM content depends on the to-be-maintained stimulus feature (Postle, 2006) as well as the goals of the experimental condition (Lee et al., 2013). However, while the topography of brain regions that retain specific stimulus features has been thoroughly investigated (for a review see Christophel et al., 2017), the influence of top-down task-demands on the localization of WM representations is less well understood.

One means by which to investigate the influence of task-demands is by employing categories or groups of stimuli. The act of categorizing a stimulus abstracts the WM representation away from the stimulus' physical features to a label or exemplar (Seger and Miller, 2010). Previous work, wherein non-human primates (NHPs) were trained to categorize images of gradual transitions between cats and dogs found that neurons in the lateral intraparietal cortex (LIP), analogous to the human intraparietal sulcus (IPS, Grefkes and Fink, 2005), represented the categorical decision instead of a continuous change with the stimulus feature (Freedman et al., 2001). Moreover, LIP neurons have also been shown to change their categorical firing pattern with changing category definitions (Freedman and Assad, 2006), known as adaptive coding (Duncan, 2001). Recently, an optogenetic study in mice went a step further and showed that parietal neurons are necessary for learning new olfactory category boundaries and generalizing from category exemplars to novel stimuli (Zhong et al., 2019).

While extensive work has been done exploring visual categorization in NHPs (Fitzgerald et al., 2011; Fitzgerald et al., 2012; Freedman and

* Corresponding author.
E-mail addresses: lisa.velenosi@fu-berlin.de (L.A. Velenosi), yuanhao.wu@nyulangone.org (Y.-H. Wu), titoschmi@zedat.fu-berlin.de (T.T. Schmidt), felix.blankenburg@fu-berlin.de (F. Blankenburg).

https://doi.org/10.1016/j.neuroimage.2020.117146
Received 6 August 2019; Received in revised form 3 July 2020; Accepted 4 July 2020
Available online 11 July 2020

Assad, 2016; Freedman et al., 2001; Sarma et al., 2016; Swaminathan and Freedman, 2012), the generalizability of the findings to other modalities is poorly understood. Rossi-Pool et al. (2016) adapted the classic delayed-match-to-sample (DMTS) comparison paradigm to explore the neuronal response of somatosensory categorical-match decisions in NHPs. The researchers recorded from primary somatosensory (SI) and premotor cortices (PMC) and found distinct neuronal firing patterns for the respective WM categories in the PMC. Moreover, a recent study using whole-brain multivariate pattern analysis (MVPA) of human fMRI data identified perceptual categories of vibrotactile stimulation in the PMC (Malone et al., 2019). Interestingly, also using MVPA with fMRI data, supramodal auditory and somatosensory category representations were identified in the IPS (Levine and Schwarzbach, 2017). Thus, somatosensory categorical-information has been consistently identified in the IPS and PMC. The present study was designed to extend this finding by identifying brain regions which maintain somatosensory WM representations in a context-dependent manner.

To this end, we defined four stimuli, composed of different pulse sequences similar to those employed by Rossi-Pool et al. (2016), which participants were pseudorandomly trained to pair together into two groups of two stimuli. We used a DMTS paradigm with two conditions: a Stimulus condition where participants were instructed to maintain only the temporal nature of the cued stimulus, and a Group condition where participants maintained the cued stimulus' group. Using a multivariate ANOVA approach (MANOVA, Allefeld and Haynes, 2014) with human fMRI data, we first identified regions maintaining condition-general stimulus-specific WM information and, in a second step, identified context-dependent group-specific WM information. We hypothesized that our experimental manipulation, maintaining individual stimuli in the Stimulus condition as opposed to groups of stimuli in the Group condition, would result in the condition-dependent modification of the multivariate WM representations, such that, in the Group condition, the group members' representations would be more similar to one another than in the Stimulus condition.

2. Materials & methods

2.1. Participants

In total, data from 38 participants was collected and two were excluded from the analysis due to low task performance, which was defined as a mean performance on either condition, Stimulus or Group, two standard deviations below the group mean. The final data set consisted of 36 participants between the ages of 20 and 39 (mean 26.92 ± 4.66 (SD) years, 19 male and 17 female). All participants provided written informed consent to take part in the study which was approved by the Ethics Committee of the Freie Universität Berlin and corresponded to the Human Subject Guidelines of the Declaration of Helsinki.

2.2. Procedure

The experiment took place across two sessions: training and fMRI data collection. The training session was used to determine the participant's sensory threshold and to adjust the subjective amplitude as well as familiarize participants with the stimuli (detailed in 2.3) and the experimental procedure (detailed in 2.4).

The training session lasted between 40 min to an hour. First, the participant-specific stimulation intensity was determined by estimating the participant's subjective detection threshold (mean: 2.33 mA ± .75 (SD)). The chosen amplitude, about double the detection threshold, was always below the participant's motor and pain thresholds resulting in a mean factor increase of 2.13 (± .50). Next, the four experimental stimuli were presented to the participant. The participant was able to freely replay each of the stimuli until they felt confident that they could differentiate the stimuli. The participant was then taught their assigned grouping. The groupings were introduced by playing the group members one after another and then participants were able to freely replay the grouped stimuli. To ensure participants had learned their assigned grouping, two stimuli were chosen at random and the participant indicated whether they belonged to the same group. This was repeated ten times. Next, the participant completed one block of each experimental condition (see 2.4). Performance above 80% on all of the behavioural tests was used to determine whether participants could perform the task. The training session thus served to familiarize participants with the stimuli, groupings and trial structure, including their assigned response and cue-mappings.

2.3. Stimuli & groupings

Stimuli were presented to the participant's left median nerve using a Digitimer DS7A constant current neurostimulator (Digitimer Ltd, Hertfordshire, UK) with MR-compatible adhesive electrodes (GVB-geliMED GmbH, Bad Segeberg, Germany). Four stimuli, each consisting of a different pulse sequence lasting 0.75 s, were created and used for all participants (Fig. 1A). The stimuli were composed of four 50 μs pulses with two of the pulses marking the on- and offset of each stimulus. The timing of the two remaining pulses was chosen to create a stimulus set with similar differentiability and performance rates across the stimuli, as assessed using behavioural pilot data. Stimuli were presented using custom MATLAB code (R2013b, The MathWorks, Inc., Natick, Massachusetts, United States) and the Psychophysics Toolbox extension (Brainard, 1997).

Each participant was pseudorandomly assigned a grouping. For four stimuli, three permutations of two groups of two stimuli exist (1) group A: s1 + s2 vs group B: s3 + s4, 2) A: s1 + s3 vs B: s2 + s4, and (3) A: s1 + s4 vs B: s2 + s3). To protect against potential naming confounds, three additional groups were included with the group A vs group B label exchanged (4) group A: s3 + s4 vs group B: s1 + s2, etc.). Therefore, six stimulus groupings were used in total, and each was pseudorandomly assigned to six participants. Arbitrary groupings were implemented because, while neurophysiological recordings can dissociate categorical from stimulus feature-specific neuronal activity, the distinction is more nuanced with fMRI data. Rule-based categorization, wherein categories are formed by applying a rule to stimulus features, is inherently coupled with the neuronal response to the underlying features. This is in contrast to arbitrary categorization, which we refer to as grouping, which classifies stimuli without the use of a stimulus-based rule (Seger and Miller, 2010). Consequently, a group can consist of physically unrelated members whereas category members share common features. Therefore, the use of arbitrary groups of stimuli, where groups are not defined according to physical attributes, provides a means of exploring the effect of task-demands on WM stimulus representations while maintaining the ability to dissociate condition-effects from stimulus features with neuroimaging data, a technique that has previously been employed in visual (Li et al., 2007; Fitzgerald et al., 2011; Senoussi et al., 2016) and audiotactile (Levine and Schwarzbach, 2018) studies.

2.4. Experimental conditions and design

The experiment comprised two independent blocks of WM conditions: Stimulus and Group. The trial timing and structure was identical in the two conditions and each experimental run consisted of one Stimulus and one Group block of trials (Fig. 1B). Each trial began with the sequential presentation of two different 0.75 s stimuli with a 0.5 s inter-stimulus-interval. Stimuli from the same group were never presented together in a trial. Additionally, during stimulus presentation, the fixation cross increased in brightness to help participants attend to the stimulus as well as ensure that the on- and offset of each stimulus was well defined. A 0.5 s visual retro-cue, square or diamond, presented after the second stimulus, indicated which of the two stimuli should be maintained in WM for the following 7.5 s delay period. In the Stimulus trials, participants were instructed to maintain only the cued stimulus. A

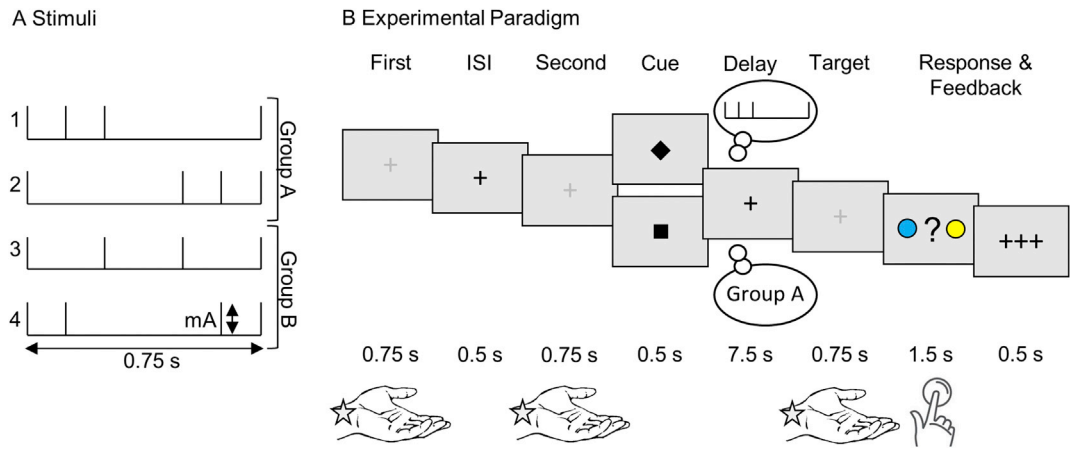

Fig. 1. Experimental Design. A. Visual depiction of the tactile stimuli used in the study. Four 0.75 s duration stimuli, each composed of four 50 μs electrical pulses and participant-specific amplitude (mA), with different stimulation pulse timings were used. The stimuli were pseudorandomly grouped into two groups of two stimuli, with group assignment balanced across participants. Six different groupings were used, for example: group A = stimulus 1 + 2 vs group B = stimulus 3 + 4. **B.** The design consisted of two blocks of conditions: Stimulus and Group. For both conditions, each trial began with the sequential presentation of two different stimuli. A visual retro-cue indicated which stimulus should be maintained in WM during the delay period. In the Stimulus trials, participants maintained only the cued stimulus, whereas in the Group trials they were instructed to maintain the group which the cued stimulus belonged to. An example of the WM content is shown for the Stimulus trials in the thought bubble above the experimental paradigm, and below for the Group trials. After the delay, participants indicated with a button response whether a target stimulus matched the maintained stimulus (Stimulus trials) or was a member of the same group (Group trials). Visual feedback was provided after each trial.

target stimulus, one of the four experimental stimuli, was presented after the delay. In the Stimulus condition, participants decided whether the target stimulus was identical to the maintained stimulus. In contrast, in the Group condition, participants were instructed to maintain the group to which the cued stimulus belonged in WM and indicated whether the target was either the cued stimulus or it's group member. Thus, the target-specific decision and response differed between the two conditions.

For both conditions, the correct target, meaning the target matching the cued stimulus, or the cued-stimulus' group member in the Group condition, was presented in 50% of trials. After the target was presented, a question mark replaced the fixation cross and a yellow and blue circle appeared on either side. Participants indicated whether the target was a match to the cued stimulus by selecting, via button press using the right index or middle finger, either the blue or yellow circle according to a pseudorandomly-defined response mapping. The response period was limited to 1.5 s. The quick response encouraged participants to actively keep the maintained stimulus or group in WM, thereby allowing a fast comparison to the target stimulus. Feedback was provided after each trial. Importantly, we implemented retro-cues (shapes) to dissociate perceptual processes from WM content as well as unpredictable response colour-map locations (left, right) to prevent a direct mapping between WM content and the decision. Furthermore, we counter-balanced the retro-cues and response choices across participants.

For each participant, four fMRI runs of experimental data were collected. Each run consisted of one Stimulus and one Group condition block, the order of which was counter-balanced across runs for each participant and was verbally communicated to the participant at the beginning of each run. The transition between blocks was indicated by the visual presentation of the mean performance on the first block, followed by the fixation cross for 12 s before beginning the second block. Moreover, we ensured that participants performed the correct task by monitoring their performance and asking after each run. The conditions consisted of identical trials, meaning that we presented the same stimulus pairings in each condition, and the trial order was randomized separately. In each condition, participants remembered each stimulus eight times, resulting in a total of 32 trials/condition (8 repetitions x 4 stimuli) and 64 trials/run (32 trials x 2 conditions). A trial lasted 12 s and inter-trial intervals (2 or 4 s) were equally distributed across trials. A run lasted 15 min. Finally, after data collection was completed, participants underwent a debriefing session wherein they drew a portrayal of the stimuli and explained the approach they used to represent the stimuli and groups.

2.5. Data acquisition

Functional imaging was performed on a 3T Siemens Tim Trio system (Siemens Medical Solutions, Erlangen, Germany) equipped with a 32-channel head coil at the Centre for Cognitive Neuroscience Berlin. 475 volumes were acquired in each of the four experimental runs using a gradient-echo echoplanar T2*-weighted imaging sequence (TR = 2000 ms, TE = 30 ms, 37 contiguous slices, ascending order, gap = 20%, matrix size = 64 × 64, 3 × 3 × 3 mm^3, flip angle = 70°, FOV = 192 mm). Additionally, a T1-weighted, whole-brain structural scan was obtained using a Magnetization Prepared Rapid Gradient Echo sequence (TR = 1900 ms, TE = 2.52 ms, 176 slices, matrix size = 256 × 256, 1 × 1 × 1 mm^3, flip angle = 9°, FOV = 256 mm). Furthermore, we implemented 'delay-locked' acquisition timing, wherein the onset of the retro-cue coincided with the onset of a volume acquisition. Delay-locking ensures that a given slice is always measured at the same time relative to the experimental paradigm (Christophel et al., 2012; Schmidt et al., 2017).

2.6. fMRI data analysis

All data analyses were performed using SPM12 (Wellcome Trust Centre for Neuroimaging, Institute for Neurology, University College London, London, UK) in combination with the cvMANOVA Toolbox (Allefeld and Haynes, 2014) and custom MATLAB code (R2013b, The MathWorks, Inc., Natick, Massachusetts, United States; code available upon request). We hypothesized that our experimental manipulation, maintaining individual or groups of stimuli in WM, would result in the context-dependent modification of WM information such that the multivariate representations of grouped stimuli should be more similar to one another in the Group condition than in the Stimulus condition. To identify differences between WM representations across conditions, we took advantage of the cvMANOVA's ability to perform interaction analyses in multivariate space. All reported coordinates correspond to MNI space and, where possible, the SPM anatomy toolbox was used to establish cytoarchitectonic references (Eickhoff, 2007). The brain figures were made using MRIcron (www.nitrc.org).

2.6.1. Data pre-processing

A 1/192 Hz high pass filter was used to remove slow varying trends in the data. To preserve the spatiotemporal structure of the data for the cvMANOVA, pre-processing was limited to slice-time correction and motion-correction, wherein images are initially realigned to the first image and then to the mean using six parameter rigid body transformation, to reduce slice order and movement-related artefacts. Functional images were normalized to standard MNI space using SPM's unified segmentation. Structural images were coregistered to the mean functional image.

2.6.2. First-level models

General Linear Models (GLMs) were defined for each participant to yield run-wise beta estimates of voxel-wise activation for the regressors of interest. First, we defined a regressor for each cued stimulus for each condition separately (4 stimuli x 2 conditions = 8 regressors). The regressor onsets coincided with the retro-cue offset and spanned the WM delay period. We refer to the Stimulus condition regressors as S1, S2, S3, and S4 and the associated Group condition regressors as A1, A2, B3, and B4. The regressor label indicates the stimulus number (1:4) as well as the associated group (A, B). Importantly, the regressors for both conditions, Stimulus and Group, were defined according to the participant-specific grouping. Thus, the regressors S1 and A1 refer to the same physical stimulus in the Stimulus and Group condition respectively. Nine impulse regressors of no interest were included with the onsets defined according to the respective trial timing: stimulus perception collapsed over first and second presentation (4 stimuli), visual retro-cues (2 cues), target presentation (1) and response (2 options). Thus, each run was modelled with 17 regressors and the first level models included 72 regressors ((17 regressors x 4 runs) + 4 run constants) which were convolved with the hemodynamic response function.

2.6.3. Searchlight cvMANOVA

The resulting run-wise beta parameter estimates were used in a whole-brain searchlight, cross-validated, multivariate analysis of variance (cvMANOVA, Allefeld and Haynes, 2014) which allowed the identification of WM information in a spatially-unbiased manner (Kriegeskorte et al., 2006). Analogous to well-established multivariate decoding methods such as support vector machines, the cvMANOVA identifies brain regions which show a difference between the multivariate BOLD activation patterns for contrasted stimuli. In the present study, the cvMANOVA was chosen instead of other multivariate decoding methods for a number of reasons. First, the cvMANOVA provides a parameter-free analysis built on a data-specific probabilistic model. Second, the resulting pattern distinctness value (Ds) directly estimates the amount of multivariate variance accounted for by the contrast. Thus, the pattern distinctness value indicates the dissimilarity of, in the present case, the contrasted WM representations. Third, and most importantly, the cvMANOVA enables interaction analyses to be performed in multivariate space which is not possible using classifiers (for a more in-depth description, see Allefeld and Haynes, 2014).

Using the cvMANOVA toolbox (https://github.com/allefeld/cvmanova), a 4-voxel radius searchlight was defined (~257 voxels) which delineated which voxels would be included in the analysis. The run-wise beta estimates for voxels contained within the searchlight were then fit with a multivariate normal distribution for each contrasted condition separately (e.g. S1 – S2). The pattern distinctness is defined as the magnitude of the covariance between contrasted conditions normalized with respect to the error covariance. Thus, the pattern distinctness estimates the amount of variance which can be explained by the contrast, measured in error variance units (Allefeld and Haynes, 2014). In other words, the larger the pattern distinctness, the more variance is accounted for by the contrast, the more distinctive the WM representations. Moreover, we employed a cross-validation approach wherein data from three of the four runs were used to fit the multivariate normal distributions and the remaining data were used to test the generalizability of the fit. This cross-validated, pattern distinctness estimate (Ds) was recorded as the value at the centre of the searchlight. The searchlight then progressed, voxel by voxel, through the brain producing a participant-specific, whole-brain pattern distinctness image for the contrast of interest. A whole-brain searchlight analysis was performed because, while we had a strong a priori hypothesis regarding the cortical regions (IPS, PMd), mainly from NHPs, the relevant subregions were unknown.

2.6.4. Stimulus-specific WM information

First, for each participant, we performed pair-wise stimulus contrasts to identify brain regions maintaining stimulus-specific WM information in both, Stimulus and Group, experimental conditions. To ensure that the cvMANOVA identified stimulus-specific information and not information relating to the different experimental conditions, stimuli in each condition were first contrasted separately and a second level conjunction analysis (Nichols et al., 2005) was used to identify stimulus-specific WM information across both conditions (explained in detail below). Moreover, to ensure that the identified information related to the cued and not the uncued stimulus on each trial, pair-wise contrasts were performed on a specific set of stimulus comparisons. The experimental design comprised trials where stimuli from the same participant-specific group were never presented together (i.e., A1 and A2 or B1 and B2). Thus, on trials when A1 was cued to be maintained in WM, B3 or B4 was the uncued stimulus. The same is true for trials where A2 was cued: B3 or B4 was uncued. Thus, regressors for A1 and A2 (and B3 and B4) were defined using trials where the cued stimulus differed (A1 or A2) but the uncued stimuli are the same within a regressor (B3, B4). We refer to these regressors as matched with respect to the uncued stimuli. Consequently, regressors for A1 and B3 were not matched with respect to the uncued stimuli. The same was true for the Stimulus condition: S1 and S2, S3 and S4 are matched for the uncued stimuli. To ensure that the WM information was specific to the cued stimuli and not confounded by activation relating to the uncued stimuli, only regressors matched for the uncued stimuli were contrasted (condition-specific contrast matrices: Ds(Stimulus condition) = mean([(S1 – S2), (S3 – S4)]), Ds(Group condition) = mean([(A1 – A2), (B3 – B4)]). Thus, the stimulus-specific WM analysis identified brain regions with pattern distinctness estimates greater than zero ($Ds > 0$). Thereby identifying regions with multivariate representations for contrasted stimuli in the Stimulus and Group conditions respectively. The complete contrast matrices are provided in the Supplemental Table 1a.

The resulting whole-brain, participant-specific pattern distinctness (Ds) images for both the Stimulus and Group condition contrasts were normalized to MNI space, smoothed with an 8 mm FWHM kernel and entered into a second-level repeated-measures ANOVA. A conjunction across the two experimental conditions identified brain regions maintaining condition-general stimulus-specific WM information ($Ds > 0$) regardless of the experimental task demands (Ds(Stimulus-specific) = mean([(S1 – S2), (S3 – S4)]) ∩ mean([(A1 – A2), (B3 – B4)]).

All statistical maps were thresholded at $p < 0.05$ family-wise error (FWE) corrected at the cluster level with a cluster-defining threshold of $p < 0.001$. In SPM, FWE correction relies on random field theory assuming smooth spatial maps of activation (for a description see Ostwald et al., 2019).

2.6.5. Context-dependent WM information

Next, as the core test of group-specific WM, we identified brain regions maintaining context-dependent WM information. We hypothesized that our experimental manipulation, forming groups of stimuli in the Group condition, would result in the modification of the multivariate representation of stimuli from the same group such that the stimuli share a more similar WM representation in the Group condition than in the Stimulus condition. Thus, the experimental manipulation should result in an interaction across conditions such that the pattern distinctness estimates between group members should differ in the two conditions (Ds(Group condition) < Ds(Stimulus condition)). Note, it is insufficient

to identify group-specific WM information by contrasting the groups against one another ([A1, A2] - [B3, B4]) because the groups were composed of physically distinct stimuli. Thus, contrasting group A against group B would identify a mixture of stimulus- and group-specific WM information. Instead, to isolate context-dependent, group-specific information, we performed an interaction analysis across the Stimulus and Group conditions (interaction contrast matrix Ds(interaction) = mean([(A1 – A2) – (S1 – S2)], [(B3 – B4) – (S3 – S4)]). Importantly, analogous to the stimulus-specific WM analysis, this interaction only contrasts regressors which were matched for the respective uncued stimuli. The complete contrast matrix is provided in the Supplemental Material Table 1b. Analogous to the stimulus-specific WM information, the resulting whole-brain, interaction pattern distinctness contrast images were normalized to MNI space and smoothed with an 8 mm FWHM kernel. Participant-specific images were forwarded to a second level one-sample *t*-test against zero to identify brain regions containing context-dependent group-specific WM representations.

As an additional step to visualize the interaction results, we plotted the mean participant-specific, context-dependent pattern distinctness values obtained for each condition (Ds(Stimulus condition) = mean([S1 – S2, S3 – S4]); Ds(Group condition) = mean([A1 - A2, B3 – B4]) from the whole-brain searchlight group-level interaction result peaks.

2.7. Control analyses

2.7.1. Group representation control analysis

While the interaction analysis indicates a differential representation of the stimuli across the two experimental conditions, it does not warrant the presence of a group representation in the Group condition. It is possible that, instead of being represented according to group membership, all stimuli are represented more similarly in the Group condition than in the Stimulus condition. Contrasting different-group members against same-group members is the most direct method for determining whether group representations were formed in the Group condition, because grouped stimuli should share a more similar WM representation than stimuli from different groups (Ds(different-group) > Ds(same-group)). Unfortunately, this analysis is confounded. Contrasts of stimuli from different groups (i.e., A1 - B3) are unbalanced with respect to the uncued stimulus (see **2.6.4** for an explanation) resulting in an overestimation of the pattern distinctness for contrasts of stimuli from different groups.

However, with this confound in mind, we performed an additional searchlight cvMANOVA analysis to determine whether, in the Group condition, stimuli from different groups were represented more differently than stimuli from the same group. We defined four different-group contrasts (A1 - B3, A1 - B4, A2 - B3, A2 - B4) and two same-group contrast (A1 - A2, B3 - B4). Next, we extracted the pattern distinctness values for the peak voxels identified by the context-dependent WM analysis (**2.6.5**) and performed a paired *t*-test to determine whether the mean participant-specific different-group pattern distinctness values were significantly different from the same-group values.

2.7.2. Behavioural control analysis

In a second control analysis, we aimed to identify whether the neuroimaging results were driven by the observed behavioural differences across stimuli and conditions. To this end, we median-split the participants according to the participant-specific difference in performance between stimulus 3 and 4 in the Stimulus condition. We chose this definition because this was the major cause of the observed behavioural effects. The two sub-samples (n = 18) were composed of participants who either performed similarly across all four stimuli and those who performed differently. We then re-ran the stimulus-specific (**2.6.4**) and context-dependent WM analyses **(2.6.5)** for each sub-sample independently. We expected that we would be able to replicate our main findings in both sub-samples, thereby demonstrating that the observed neuroimaging results are independent of the differences in behaviour. However, if only the differently-performing sub-sample was able to reproduce the results, then the neuroimaging results were indeed driven by the difference in behavioural factors.

2.7.3. Response time control analysis

Next, we performed a control analysis to determine whether the neuroimaging results were influenced by the observed difference in response times. To this end, we defined new first level models and included an HRF-convolved parametric response time regressor of no-interest. We then repeated both the stimulus-specific **(2.6.4)** and the context-dependent WM **(2.6.5)** main analyses. We expected that we would be able to replicate our main findings, thereby demonstrating that our neuroimaging findings are independent of the observed differences in response times.

2.7.4. WM-specificity control analysis

Next, we performed a control analysis to ensure that the identified regions were specific to the stimulus in WM and not corrupted by ongoing perceptual processes. To this end, we repeated both the stimulus-specific **(2.6.4)** and the context-dependent **(2.6.5)** WM analyses with new first level models with regressors modelling the uncued stimuli. This control analysis enabled the detection of information relating to the uncued stimulus and provided a method for testing the specificity of our results.

2.7.5. Multivariate control analysis

In a final control analysis, we aimed to determine whether the identified WM information was indeed multivariate in nature, or if the neuroimaging results could be explained by mass-univariate differences between the conditions. We repeated both the stimulus-specific **(2.6.4)** and the context-dependent **(2.6.5)** analyses using a searchlight comprising only one voxel. This analysis collapsed the multivariate cvMANOVA to a single dimension and tested whether the identified WM information comprised a univariate representation.

3. Results

3.1. Behavioural results

Overall, participants performed with a mean accuracy of 81.87% (±7.59% (SD) range: 68.36–97.27%). To test for potential performance differences between experimental conditions or stimuli, we performed a 4 × 2 repeated-measures ANOVA with the stimuli (1:4) and conditions (Stimulus, Group) as within-subject factors. The ANOVA identified a significant main effect of stimulus ($F(3, 105) = 10.9367$, $p = 2.6098e\text{-}06$, $\eta^2 = 0.1207$) and condition ($F(1, 35) = 5.0929$, $p = 0.0304$, $\eta^2 = 0.0234$) and no interaction between the factors ($F(3, 105) = 2.2282$, $p = 0.0892$). Post-hoc, Bonferroni-corrected, paired t-tests of the stimulus effect revealed it to be driven by differences in performance between stimulus 1 and 3, and stimulus 4 and all other stimuli (mean performance stimulus 1: 81.38 ± 1.52% (SE), S2: 82.55 ± 1.56%, S3: 86.15 ± 1.59%, S4: 77.39% ± 1.65%; S1 vs S3: $T(35) = 3.0014$, $p = 0.0049$, Cohen's $d = 0.5116$, S1 vs S4: $T(35) = 2.9083$, $p = 0.0063$, $d = 0.4195$, S2 vs S4: $T(35) = 3.8237$, $p = 0.0005$, $d = 0.5366$, S3 vs S4: $T(35) = 4.9355$, $p < 0.0001$, $d = 0.9019$). The mean performance results across participants are shown in Fig. 2A with the stimulus labelling referring to the physical, and not participant-specific labelling. The significant differences between stimuli ($p < 0.05$, Bonferroni-corrected) are indicated by grey lines.

Participants responded with a mean of 735.1 ms ± 105.5 ms (SD), well-within the allotted 1.5 s response window. We performed a second 4 × 2 repeated-measures ANOVA using response time as the dependent variable and found a main effect of condition, with Stimulus condition response times significantly shorter than the Group condition (Stimulus mean: 663.5 ± 17.5 ms (SE), Group mean: 807.1 ± 19.4 ms, $F(1, 35) = 162.3934$, $p = 1.0436e\text{-}14$, $\eta^2 = 0.6313$), and no main effect of stimulus

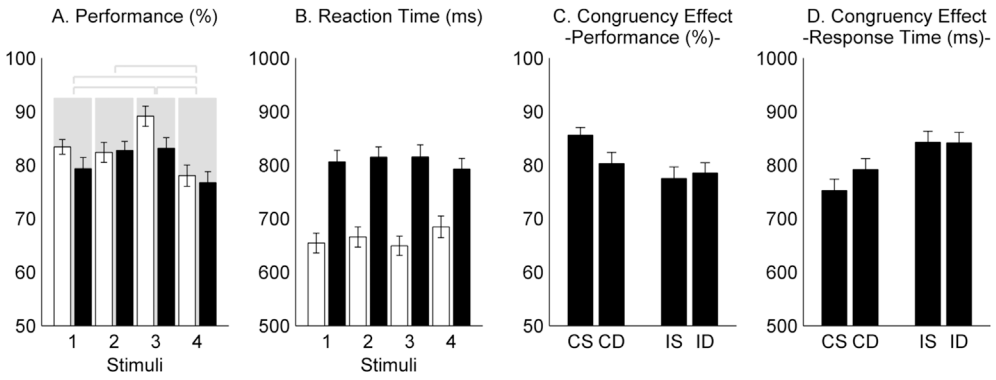

Fig. 2. Behavioural Results A. The mean behavioural performance across participants for the four stimuli, in both conditions: Stimulus (white) and Group (black). The grey brackets indicate significant differences ($p < 0.05$, Bonferroni-corrected) in performance between stimuli across conditions. **B.** The mean response time across participants for the four stimuli, in both conditions. **C.** The mean performance across participants in the Group condition with trials sorted according to the relationship between the cued and target stimulus. CS: same group – same stimulus, CD: same group – different stimulus, IS: different group – 'same' stimulus, ID: different group – 'different' stimulus. **D.** Shows the same as C with response time data. In both C. and D., the CD trials are intermediate to the CS and incongruent trials suggesting that a group was maintained in the Group condition. Error bars for all plots indicate standard error of the means.

($F(3, 105) = 0.5766$, $p = 0.6316$). However, an interaction between the factors was present ($F(3, 105) = 5.9177$, $p = 9.0422e\text{-}04$, $\eta^2 = 0.0142$, Fig. 2B). The main effect of condition is expected given the Group condition required two stimuli, the two maintained group members, to be compared with the target stimulus, thereby requiring more time than the single comparison in the Stimulus condition. The influence of the observed behavioural effects on the neuroimaging results is explored in subsequent control analyses (2.7.2, 2.7.3).

Finally, we investigated whether participants performed according to the experimental manipulation and represented groups in the Group condition. We theorised that grouping the stimuli would influence the congruency effect by creating an intermediate level between congruent trials (target is identical to cued stimulus) and incongruent trials (target is not the cued stimulus). To test this, we defined two independent 2×2 repeated measure ANOVAs for the performance and response time data with factors congruency (target stimulus from the same group as cued stimulus or different group) and stimulus identity (same or different stimulus from cued). Thus, the ANOVAs were composed of four cells: congruent-same stimulus (CS: e.g. cued A1 – target A1), congruent-different stimulus (CD: cued A1 – target A2), incongruent-'same' (IS), incongruent-'different' (ID). For the IS and ID cells, the trials (cued A1 - target B3 or B4) were equally divided between the two levels. Each trial type (B3 or B4 as target) was repeated twice in each experimental run. Thus, the IS cell comprised the first trial-instance and the ID cell the second. The performance data ANOVA identified a main effect of congruency ($F(1, 35) = 13.9126$, $p = 6.7655e\text{-}04$, $\eta^2 = 0.1169$), no effect of group-member identity ($F(1, 35) = 3.3718$, $p = 0.0748$), and an interaction between the factors ($F(1, 35) = 5.8944$, $p = 0.0205$, $\eta^2 = 0.0488$; Fig. 2C). The response time data replicated the performance data results with the addition of a main effect of stimulus identity which, as seen in Fig. 2D, is the result of the near-identical response times on incongruent trials (congruency: $F(1, 35) = 52.6285$, $p = 1.7985e\text{-}08$, $\eta^2 = 0.4343$; group-member identity: $F(1, 35) = 9.1019$, $p = 0.0047$, $\eta^2 = 0.0315$; interaction: $F(1, 35) = 14.2528$, $p = 5.9488e\text{-}04$, $\eta^2 = 0.0359$). Thus, trials when the target stimulus was a group-member of the cued stimulus were intermediate in performance and response time to congruent and incongruent trials, thereby providing evidence for participants having likely maintained groups in the Group condition.

3.2. Neuroimaging results

3.2.1. Stimulus-specific WM information

Using the whole-brain, searchlight cvMANOVA, we identified regions maintaining stimulus-specific WM information in the Stimulus and Group experimental conditions respectively (condition-specific results are shown in Supplemental Figure 1). Moreover, to ensure that the results are independent from the uncued stimuli, we contrasted pairs of regressors which were matched for the uncued but differed with respect to the maintained (cued) stimulus. Because we were interested in regions which maintain stimulus-specific WM information across experimental conditions, we performed a second-level conjunction analysis (logical AND, Friston et al., 2005) across the two experimental conditions to identify regions which maintain context-general, stimulus-specific WM (Fig. 3A (blue), Table 1a). This analysis identified a cluster in the left inferior frontal gyrus (IFG) extending to the middle frontal gyrus (MFG) as well as a cluster in the left superior parietal lobule (SPL) as maintaining stimulus-specific WM information independent of experimental context.

3.2.2. Context-dependent WM information

We hypothesized that our experimental manipulation, grouping stimuli in the Group condition and treating them as individuals in the Stimulus condition, would result in the context-dependent modification of the group members' pattern distinctness estimates. We expected a smaller difference between the multivariate WM representations of the grouped stimuli in the Group as compared to the Stimulus condition ($Ds(\text{Group condition}) < Ds(\text{Stimulus condition})$). Therefore, regions which maintain context-dependent group-specific WM information should display different pattern distinctness estimates between group members across the two conditions, which is accessible with an interaction analysis (see **2.6.5**). Moreover, because the implemented interaction only contrasts physically identical pairs of stimuli while also controlling for the uncued stimuli (see **2.6.4**), the contrast is not confounded by stimulus feature information. The interaction contrast identified the left IPS (Fig. 3A (yellow), Table 1b). Thus, the WM representations of the grouped stimuli in the left IPS are represented differently in the two conditions, or put another way, the left IPS adaptively modifies its WM information with respect to the experimental condition. Additionally, due to strong a priori expectations regarding the presence of group-specific somatosensory information in the PMC (Malone et al., 2019; Rossi-Pool et al., 2016, 2017, 2019), we further explored the interaction contrast result and identified context-dependent WM representations in the left PMd at an uncorrected threshold ($p < 0.001$). Other regions with effects detectable at this threshold included the right middle frontal gyrus, left inferior frontal gyrus, left premotor cortex and the cluster in the left intraparietal sulcus extending from the superior parietal lobule to the angular gyrus (see the unthresholded statistical maps at Neurovault: https://identifiers.org/neurovault.collec

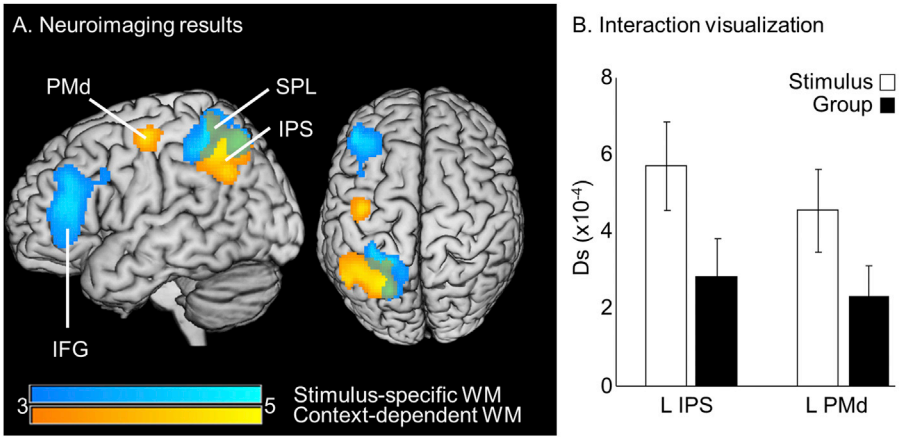

Fig. 3. Neuroimaging cvMANOVA results A. We identified brain regions which maintain condition-general stimulus-specific (blue) and context-dependent group-specific (yellow) WM information with overlapping regions shown in green. Using a conjunction analysis across the Stimulus and Group condition results, we identified condition-general stimulus-specific WM information in the left IFG and SPL whereas context-dependent WM information was identified in the left IPS. Results are reported at $p < 0.05_{FWE}$ with $p < 0.001_{cluster}$. The left PMd cluster was significant at, and shown at, an uncorrected threshold ($p < 0.001$). Coloured bars indicate the respective voxel-wise T-statistic values. PMd: dorsal premotor cortex, SPL: superior parietal lobule, IPS: intraparietal sulcus, IFG: inferior frontal gyrus. **B.** To visualize the interaction, we extracted the mean pattern distinctness values across participants at the context-dependent WM analysis peaks (L IPS, L PMd) for the two experimental conditions (Stimulus, Group). The error bars indicate the standard error of the means. Unthresholded group contrast images for the Stimulus and Group condition stimulus-specific and context-dependent WM results are available on Neurovault (https://identifiers.org/neurovault.collection:5623).

Table 1
Neuroimaging results overview. **1a**. Regions maintaining stimulus-specific WM information independent of experimental context as revealed by a conjunction analysis. **1b**. Regions maintaining context-dependent WM information as revealed by an interaction analysis. For both Table 1a and b, the Anatomy Toolbox (Eickhoff, 2007) was used, where possible, to establish the label and the x, y, z coordinates refer to MNI space. The T-stat value refers to the peak voxel in the cluster with size k. Ds is the cross-validated pattern distinctness estimate with 1a referring to the mean Ds across the two conditions and 1b referring to the interaction contrast value.

Table 1a: Stimulus-specific WM information						
Label	X	Y	Z	T-stat	k	Ds x 10^{-4}
L IFG	−42	36	14	4.76	1373	8.0137
L SPL	−22	−48	60	4.74	1071	6.7954
Table 1b: Context-dependent group-specific WM information						
L IPS	−26	−66	54	5.09	1441	7.6486
L PMd	−42	−12	58	4.39	207	6.4042

tion:5623).

We additionally visualized the two halves of the interaction analysis, the Stimulus and Group condition, for the peaks identified by the whole-brain, context-dependent searchlight analysis (L IPS, L PMd, Fig. 3B). As expected, the pattern distinctness estimates for grouped stimuli are smaller in the Group condition than in the Stimulus condition, indicating that the IPS represented grouped stimuli more similarly in the Group condition than in the Stimulus condition.

3.3. Control analyses results

3.3.1. Group representation control analysis results

To ensure that the context-dependent WM analysis identified groups in the Group condition and not condition-general changes in pattern distinctness, we performed a control analysis to test whether grouped stimuli were represented more similarly in the Group condition than stimuli from different groups. In the IPS, the grouped stimuli were more similarly represented than stimuli from different groups (same-group mean: 2.8334e-04 ± 0.9532e-04 (SE); different-groups mean: 5.6038e-04 ± 1.1092e-04; T(35) = 2.6518, p = 0.0119, Cohen's d = 0.4465). Whereas there was no evidence of stimulus grouping in the PMd (same-group mean: 2.3017e-04 ± 0.8008e-04, different-groups mean: 3.4602e-04 ± 0.8626e-04; T(35) = 1.6302, p = .1120). Thus the IPS and not the PMd represented the grouped stimuli significantly more similarly than stimuli from different groups in the Group condition.

3.3.2. Behavioural control analysis results

In a second control analysis, we aimed to identify the influence of the behavioural effects on the neuroimaging results. To this end, we median-split the participant sample according to the performance difference between stimuli resulting in two sub-samples: similarly- (SIM) and differently-performing participants (DIF). For the SIM sub-sample, the 4 × 2 ANOVA on performance data identified no main effect of stimulus ($F(3,51) = 0.7833$, $p = 0.5088$), no effect of condition ($F(1,17) = 3.6479$, $p = 0.0732$) and no interaction between the factors ($F(3,51) = 0.8678$, $p = 0.4639$). Moreover, the 4 × 2 ANOVA on response time data identified a large condition effect ($F(1,17) = 82.8068$, $p = 6.0569e-08$, $\eta^2 = 0.6579$) and no stimulus effect ($F(3,51) = 0.3274$, $p = 0.8055$) or interaction between the factors ($F(3,51) = 1.6130$, $p = 0.1978$). Thus we were able to remove all but the condition difference in response times (addressed in **2.7.3**). The neuroimaging results for the SIM sub-sample identified a cluster overlapping with the left SPL cluster in the stimulus-specific WM analysis (peak: −22, −50, 62, T-statistic = 2.65) and in the left IPS in the context-dependent WM analysis (peak: −26, −64, 54, T-statistic = 2.40).

Next, we performed the same analysis with the differently-performing sub-sample. In contrast to the SIM sub-sample, the 4 × 2 ANOVA on the performance data identified a main effect of stimulus ($F(3,51) = 22.4457$, $p = 2.1093e-09$, $\eta^2 = 0.3191$), no effect of condition ($F(1,17) = 1.8571$, $p = 0.1907$) but an interaction between the factors was present ($F(3,51) = 6.3505$, $p = 9.6535e-04$, $\eta^2 = 0.0722$). Moreover, the 4 × 2 ANOVA on response time data identified a large condition effect ($F(1,17) = 76.2258$, $p = 1.0885e-07$, $\eta^2 = 0.6047$), no stimulus effect ($F(3,51) = 2.2522$, $p = 0.0934$) and an interaction between the factors ($F(3,51) = 6.8480$, $p = 5.7756e-04$, $\eta^2 = 0.0315$). Once again, we identified clusters overlapping with those identified in the main analyses. The left SPL contained stimulus-specific WM information (peak: −22, −50, 56, T-statistic = 5.09) whereas the left IPS contained context-dependent WM information (peak: −24, −62, 50, T-statistic = 5.22). The greater T-statistics observed with the differently-performing sub-sample, combined with our ability to replicate our findings with both sub-samples, suggests that the effect identified in the IPS might result from the combination of context-dependent WM amplified by task-difficulty.

3.3.3. Response time control analysis results

Thirdly, to identify whether the observed condition-difference in response times influenced the neuroimaging results, we reproduced the main analyses results with new first level models including an additional parametric response time nuisance regressor. We identified stimulus-specific WM information in the left SPL (peak −22, −48, 60, T-statistic = 4.69) and IFG (peak −40, 36, 14, T-statistic = 4.69) and context-dependent WM in the left IPS (peak −24, −66, 54, T-statistic = 5.06). Thus suggesting that the neuroimaging results are independent from the observed differences in response times.

3.3.4. WM-specificity control analysis results

To ensure that the results are specific to WM information, we performed a control analysis wherein we repeated the two main analyses, stimulus-specific (**2.6.4**) and context-dependent WM (**2.6.5**), with regressors defined for the uncued stimuli. The analyses did not identify any region with uncued stimulus-specific WM information even at an uncorrected threshold of $p < 0.001$ and did not identify any region showing an interaction across conditions at the corrected significance threshold. Therefore, both the stimulus-specific regions as well as the context-dependent group-specific regions are indeed maintaining information which is specific to WM.

3.3.5. Multivariate control analysis results

Finally, we tested whether the identified WM representations are multivariate in nature. To this end, we repeated the stimulus-specific (**2.6.4**) and context-dependent WM analyses (**2.6.5**) using a single voxel instead of the 4-voxel radius searchlight. Neither the stimulus-specific nor the interaction analysis identified any significant clusters of univariate WM content at the corrected statistical threshold, thereby demonstrating that the WM representations are multivariate in nature.

4. Discussion

Using whole-brain fMRI in humans in combination with the cross-validated, searchlight, multivariate ANOVA, we explored which brain regions maintain WM representations of individual and groups of somatosensory pulse sequences. In a first step, we identified the left IFG and SPL as maintaining stimulus-specific information in WM, across experimental conditions. Next, by comparing the differences in pattern distinctness across conditions, where participants were asked to maintain either an individual stimulus or group-information in WM, we identified an interaction between conditions in the left IPS (and in the left PMd at an uncorrected threshold). Moreover, in the left IPS, group members shared a more similar multivariate WM representation in the Group than in the Stimulus condition. Thus, our results suggest that the left IPS contains context-modulated WM information such that the stimuli from the same group are more similarly represented in the Group condition than in the Stimulus condition. Accordingly, our results provide additional insight into the adaptive coding ability of the parietal cortex, where task-demands influence WM representations.

4.1. Stimulus-specific WM representations

The present study identified condition-general stimulus-specific WM content within the left IFG and SPL. Moreover, we revealed that the WM representations maintained in the IFG and SPL are both specific to the cued WM content and employ a multivariate code. The identified stimulus-specific WM regions are well in line with previous findings which suggest that the IFG and SPL are capable of maintaining a wide-range of features in WM (Christophel et al., 2017; Sreenivasan & D'Esposito, 2019). Using the well-established vibrotactile WM paradigm, frequency-specific WM information has been identified in human (Schmidt et al., 2017; Spitzer et al., 2010) as well as NHP IFG (Romo et al., 1999). Moreover, experiments employing trains or sequences of stimuli, similar to those used in the present study, have shown that the IFG is involved in the perception of visual sequences (Cavdaroglu and Knops, 2018) and the maintenance of auditory sequences in WM (Uluç et al., 2018). Notably, a majority of participants (83.3%) reported in the debriefing session having remembered the stimuli by mentally verbalizing or internally singing the stimuli, thus it is not surprising that the left IFG, which is known to be involved in language production (Binder et al., 1997) and has been shown to maintain roman characteristic-specific WM content (letters) in WM (Polanía et al., 2011), maintained stimulus-specific WM information in the present study. In agreement with our results, Polanía and colleagues also found evidence for WM letter representations in the left posterior parietal cortex. The posterior parietal cortex, or SPL more specifically, has previously been shown to maintain a wide variety of WM information including locations (Jerde et al., 2012; Sprague et al., 2014, 2016), shapes (Christophel and Haynes, 2014a) and patterns composed of colour (Christophel et al., 2015; Christophel et al., 2012) and motion (Christophel and Haynes, 2014b). In line with this, we identified stimulus-specific WM information in the SPL using stimuli comprising temporal patterns of somatosensory pulses. Thus, it's possible that the SPL also maintains temporal patterns in addition to colour and motion patterns. However, previous studies have shown a divergence where frontal areas represent temporally-distributed stimuli and parietal regions represent spatially-distributed stimuli (Cavdaroglu and Knops, 2018). Therefore, participants likely transformed the stimulus features into a different representational code which was subsequently maintained in the SPL. Future studies which probe the nature of the WM representation are required to further explore the nature of the code maintained in the SPL. Consequently, we provide evidence for the maintenance of WM representations of somatosensory pulse sequences, independent of experimental context, in higher-order, frontoparietal regions.

4.2. Context-dependent WM representations

Next, we identified the left IPS and (found preliminary evidence for) the left dPMC as regions that modify their WM representations in response to changing task-demands. We expected that, by training participants on pseudorandom groupings, the resulting WM representations would be modulated such that representations of grouped stimuli would be more similar to each other when the task required the maintenance of the group, than when an individual stimulus was maintained in WM. Thus, using an interaction contrast, we localized WM representations which adapted to the changing task-demands in the left IPS. Moreover, because we compared the same physical pairs of stimuli across experimental conditions while controlling for the uncued stimuli, the identified adaptive WM information is independent of stimulus features and specific to the cued stimulus. This is significant because, due to the sluggish and indirect nature of the BOLD response, distinguishing between group- and stimulus-specific information is more nuanced with neuroimaging than with neurophysiological data. Thus, by contrasting identical pairs of stimuli across the two experimental conditions, we can be certain that the resulting WM information is specific to the group and not contaminated by stimulus feature-specific BOLD responses.

Additionally, to visualize the interaction, we plotted the group members' multivariate pattern distinctness estimates for the two experimental conditions separately (Fig. 3B). Due to a strong a priori hypothesis regarding the presence of group-specific WM information in the PMC (Malone et al., 2019; Rossi-Pool et al., 2016, 2017, 2019), we included a cluster in the left PMd which did not survive multiple comparison correction for completeness. This visualization illustrates that, for the left IPS and PMd, the group members were more similarly represented in the Group than in the Stimulus condition. In a control analysis, we additionally found evidence for the grouped stimuli to be represented more similarly than non-grouped stimuli in the Group condition in the left IPS but not the PMd. While this control analysis may be confounded (see **2.7.1**), these analyses provide additional evidence for the maintenance of context-dependent temporal patterns of vibrotactile

stimuli in WM in the left IPS. Of note, in the present study we employed cluster-based correction thresholding which may result in larger brain regions (e.g. the PPC) crossing the statistical threshold more easily than smaller regions (e.g. the PMd). This is however unlikely to have biased the reported results as post-hoc analyses with different searchlight radii (2 to 5 voxels) did not change the location of the identified clusters.

The finding of task-modulated WM information in the IPS is in line with previous work which has shown that representations of task-relevant features in the IPS change with task demands and difficulty (Jackson and Woolgar, 2018; Liu and Hou, 2013; Woolgar et al., 2011). Moreover, the IPS has been suggested to be an integral member of the multiple-demand or task-positive network, a network which processes and maintains features essential for the successful performance of a task, across changing task demands, and is influenced by rule complexity, memory load, attentional switching among other factors (Fedorenko et al., 2013; Wen et al., 2018). This is especially relevant for the present study. According to these studies, the effect of task-difficulty is to increase the resolution or strength of a task-relevant representation. Our results show the opposite effect. In the more difficult task, the Group condition, the representations of grouped-stimuli become more similar to one another instead of more distinct. Thus, it is evidence in favour of a group representation. To further explore the influence of task-difficulty in our data, we median-split the participant sample according to the consistency of the performance across stimuli. While we were able to replicate our findings with both sub-samples, the sub-sample with larger behavioural effects demonstrated larger neuroimaging effects. Thus, it is conceivable that the effect identified in the IPS is the result of a combination of context-dependent WM modification amplified by task-difficulty.

The central role of the IPS in grouping and categorizing stimuli across sensory domains and species has been well established (Freedman and Assad, 2016). A large body of research has been accumulated demonstrating the maintenance of categorical and group-specific WM information across stimulus modalities in the LIP, the IPS homologue in NHPs (Fitzgerald et al., 2011, 2013, 2012; Freedman and Assad, 2006, 2016; Freedman et al., 2001; Sarma et al., 2016; Swaminathan and Freedman, 2012). Furthermore, a new study has shown that the NHP IPS is necessary for the transformation of a stimulus representation into a more-abstract category label which is then passed to motor-selective neurons in the NHP IPS (Zhou and Freedman, 2019). More generally, Nieder (2012) has shown that both the LIP as well as NHP prefrontal regions represent auditory and visual percepts of number sets, tantamount to abstract numerical categories, in a supramodal fashion. Indeed, the PPC has been shown to be involved in a wide variety of abstract cognitive functions including the representation of cognitive sets (Oristaglio et al., 2006; Stoet and Snyder, 2004), numerosity (Nieder et al., 2006; Nieder and Miller, 2004; Tudusciuc and Nieder, 2007) and salience (Leathers and Olson, 2012), all of which can be considered various forms of categorization (Freedman and Assad, 2016). Recently, using optogenetics in combination with calcium imaging, the mouse PPC was shown to be central for the categorization of auditory frequencies (Zhong et al., 2019). The authors provide evidence for the stable representation of category exemplars in the PPC over several days and show that the PPC is necessary for the generalization from category exemplars to novel stimuli as well as for the updating of category boundaries. Furthermore, a recent study exploring cross-modal categorization employed an auditory and tactile delayed-match-to-category paradigm in humans, in combination with multivariate pattern analysis, and found overlapping tactile and auditory category information in the IPS (Levine and Schwarzbach, 2017). Taken together, the evidence across species provides a strong argument for the involvement of the IPS, and PPC more generally, in the categorization and grouping of stimuli. Indeed, a recent article merged the various LIP functions into a single role: the identification of behaviourally relevant stimuli (Freedman and Ibos, 2018). The authors suggest that the nonlinear nature of responses observed in LIP neurons in DMTS tasks points to the integration and comparison of incoming bottom-up signals with the specific top-down task-goals. Thus, taken across species, the IPS likely maintains WM representations indicating the current task goal, for example, the stimulus or group which is to be compared with the target at the end of the trial.

The PPC, prefrontal cortex, and PMC have been suggested to act together in a network which implements abstract cognitive computations, including categorization and grouping of stimuli (Freedman and Assad, 2016). Indeed, previous work investigating the representation of somatosensory categories also identified category-specific information in ventral human (Malone et al., 2019) and NHP PMd (Rossi-Pool et al., 2016, 2017, 2019). Importantly, both studies used explicit categorical rules on stimulus feature properties to define their categories (high vs low frequencies; same vs different stimulus) whereas, with the present study, we wanted to explore how abstract group representations, unrelated to the stimulus features and dissociated from an explicit rule, would affect the WM representations. In line with the NHP findings, we identified a trend towards a pattern distinctness difference for the group members in the two experimental conditions in the PMd. Of note, we identified smaller pattern distinctness values for the PMd than for the SPL and IPS across all analyses. Because the pattern distinctness value is an estimate of the amount of variance explained by a contrast, normalized by the error covariance, it is interpretable. However, it is difficult and ill-advised to compare across brain regions. Different regions are known to have different neural vasculature (Gardner, 2010), connectivity (Zalesky et al., 2012), and morphology (Bianchi et al., 2013), all of which may influence the hemodynamic response and recorded fMRI signal (Handwerker, Ollinger, & D'Esposito, 2004) making it difficult to compare the results across regions (for more information see Haynes, 2015).

A potentially important distinction between the present study and that of Malone et al. (2019) and Rossi-Pool et al. (2016) concerns the ability to prepare a motor decision. Traditionally, the PMC has been deemed responsible for the organization and planning of movements (Wise, 1985). Thus, one hypothesized role of the PMC in categorization suggests that the PMC maintains information relating to 'motor ideas' which may provide the basis for cognitive functions (Fadiga et al., 2000). In support of this hypothesis, the PMC has been shown to represent rules in a behaviourally relevant manner (Muhammad et al., 2006; Vallentin et al., 2012; Wallis and Miller, 2003). In the present study, participants maintained WM information and were not able to prepare a prospective motor plan as they did not know whether the target would match the maintained stimulus. Moreover, we included an additional precaution and pseudorandomly alternated the locations of the motor targets, thereby ensuring that participants could neither select a decision nor a motor plan. In contrast, Malone et al. (2019) did not require participants to respond to a target and therefore participants were able to select a motor response at the onset of the stimulus presentation. Similarly, Rossi-Pool et al. (2016) identified categorical representations in the PMd during the delay between the presentation of the target and the motor output, a timepoint when the NHPs had already made but not yet communicated their decision. Thus, the inability of participants in the present study to select a decision and prepare a motor output may have prevented the transformation of group-specific WM information in the IPS into a motor plan in the PMC. In line with this, the PMC has been implicated in the preparation of so-called virtual motor plans which can be transformed into a motor plan (Nakayama et al., 2008; Yamagata et al., 2012, Yamagata et al., 2009). Indeed, Rossi-Pool et al. (2019) recently re-analysed their data and found that, while there was category information in the PMd, the majority of neuronal variance could be explained by experimental timing. Thus, it is possible that the PMC is mainly responsible for determining the specific timing of events and coordinating the associated network regions, such as the stimulus-specific WM information in the IFG and SPL and the context-dependent, group-specific WM information in the IPS.

4.3. WM representations

Finally, by considering both the context-dependent and the stimulus-specific results together, we can speculate on the probable nature of the WM representational codes in the various regions. Regions identified by the stimulus-specific conjunction analysis, area 5A of the SPL and area 45 of the IFG, likely maintain stimulus feature information in WM independent of experimental conditions. Moreover, regions identified by the interaction analysis, the IPS and PMd, may maintain stimulus feature information only in the stimulus condition and an abstracted categorical or group label in the group condition (e.g. stimulus A1 and A2 maintained as A). This would also result in the difference in pattern distinctness estimates observed in the interaction analysis. Finally, the region identified by the overlap of the two analyses, area 7A of the SPL, likely maintains a combination of stimulus features as well as abstracted WM information in the group condition. Future studies are required to further probe the representational nature of the WM codes implemented by the different regions under various task-demands.

5. Conclusion

In conclusion, we present evidence for the maintenance of WM information in frontoparietal regions across experimental conditions wherein participants were instructed to maintain either individual or groups of somatosensory sequences. Additionally, we identified the maintenance of context-dependent, group-specific WM representations in the left IPS independent of stimulus properties in a paradigm that disentangled the WM representation from the categorical decision and the motor response. We show that the WM representations in the IPS adaptively change with task-demands such that, in the Group condition, group members are represented more similarly than in the Stimulus condition. Thus, we provide novel evidence for the adaptive nature of somatosensory WM representations in the IPS and suggest that somatosensory WM representations are maintained in the IPS in an adaptive, context-dependent manner.

Declaration of competing interest

The authors declare that the research was conducted in the absence of any commercial or financial relationship that could be construed as a potential conflict of interest.

CRediT authorship contribution statement

Lisa Alexandria Velenosi: Conceptualization, Data curation, Formal analysis, Funding acquisition, Investigation, Visualization, Writing - original draft. **Yuan-Hao Wu:** Conceptualization, Formal analysis, Investigation, Writing - review & editing. **Timo Torsten Schmidt:** Conceptualization, Writing - review & editing. **Felix Blankenburg:** Conceptualization, Formal analysis, Supervision, Writing - review & editing.

Acknowledgements

The authors would like to thank Pia Schröder for helpful discussions and Carsten Allefeld for comments on the methods and Alexander von Horst for help with the manuscript. Finally, the authors would like to extend their sincere gratitude to Reviewer 1 for significantly improving the quality of the manuscript.

Appendix A. Supplementary data

Supplementary data to this article can be found online at https://doi.org/10.1016/j.neuroimage.2020.117146.

Funding

LAV was supported by the Research Training Group GRK 1589/2 "Sensory Computation in Neural Systems" by the German Research Foundation (DFG).

Data code and availability statement

In accordance with the EU's General Data Protection Regulation we are unable to share raw fMRI data. However, unthresholded group contrast images for each result can be directly inspected on Neurovault (https://identifiers.org/neurovault.collection:5623). Analysis code is available upon request.

References

Allefeld, C., Haynes, J.D., 2014. Searchlight-based multi-voxel pattern analysis of fMRI by cross-validated MANOVA. Neuroimage 89, 345–357. https://doi.org/10.1016/j.neuroimage.2013.11.043.

Baddeley, A.D., Hitch, G., 1974. Working memory. Psychol. Learn. Motiv. 8, 47–89.

Bianchi, S., Stimpson, C.D., Bauernfeind, A.L., Schapiro, S.J., Baze, W.B., McArthur, M.J., et al., 2013. Dendritic morphology of pyramidal neurons in the chimpanzee neocortex: regional specializations and comparison to humans. Cerebr. Cortex 23 (10), 2429–2436.

Binder, J.R., Frost, J.A., Hammeke, T.A., Cox, R.W., Rao, S.M., Prieto, T., 1997. Human brain language areas identified by functional magnetic resonance imaging. J. Neurosci.: Off. J. Soc. Neurosci. 17 (1), 353–362.

Brainard, D.H., 1997. The Psychophysics toolbox. Spatial Vis. 10 (4), 433–436. https://doi.org/10.1163/156856897X00357.

Cavdaroglu, S., Knops, A., 2018. Evidence for a posterior parietal cortex contribution to spatial but not temporal numerosity perception. Cerebr. Cortex 2965–2977. https://doi.org/10.1093/cercor/bhy163. July 2018.

Christophel, Thomas B., Cichy, R.M., Hebart, M.N., Haynes, J.-D., 2015. Parietal and early visual cortices encode working memory content across mental transformations. Neuroimage 106, 198–206. https://doi.org/10.1016/j.neuroimage.2014.11.018.

Christophel, Thomas B., Haynes, J.D., 2014. Decoding complex flow-field patterns in visual working memory. Neuroimage 91, 43–51. https://doi.org/10.1016/j.neuroimage.2014.01.025.

Christophel, Thomas B., Hebart, M.N., Haynes, J.-D., 2012. Decoding the contents of visual short-term memory from human visual and parietal cortex. J. Neurosci.: Off. J. Soc. Neurosci. 32 (38), 12983–12989. https://doi.org/10.1523/JNEUROSCI.0184-12.2012.

Christophel, Thomas B., Klink, P.C., Spitzer, B., Roelfsema, P.R., Haynes, J.-D., 2017. The distributed nature of working memory. Trends Cognit. Sci. 21 (2), 111–124. https://doi.org/10.1016/j.tics.2016.12.007.

Duncan, J., 2001. An adaptive coding model of neural function in prefrontal cortex. Nat. Rev. Neurosci. 2 (November), 820–829. Retrieved from. http://www.cnbc.cmu.edu/~tai/readings/nature/duncan_code_prefrontal.pdf.

Eickhoff, S., 2007. SPM Anatomy toolbox. Neuroimage 91 (14), 1–21.

Fadiga, L., Fogassi, L., Gallese, V., Rizzolatti, G., 2000. Visuomotor neurons: ambiguity of the discharge or "motor" perception? Int. J. Psychophysiol. 35 (2–3), 165–177. https://doi.org/10.1016/S0167-8760(99)00051-3.

Fedorenko, E., Duncan, J., Kanwisher, N., 2013. Broad domain generality in focal regions of frontal and parietal cortex. Proc. Natl. Acad. Sci. Unit. States Am. 110 (41), 16616–16621. https://doi.org/10.1073/pnas.1315235110.

Fitzgerald, J.K., Freedman, D.J., Assad, J.a., 2011. Generalized associative representations in parietal cortex. Nat. Neurosci. 14 (8) https://doi.org/10.1038/nn.2878, 1075-U179.

Fitzgerald, Jamie K., Freedman, D.J., Fanini, A., Bennur, S., Gold, J.I., Assad, J.A., 2013. Biased associative representations in parietal cortex. Neuron 77 (1), 180–191. https://doi.org/10.1016/j.neuron.2012.11.014.

Fitzgerald, Jamie K., Swaminathan, S.K., Freedman, D.J., 2012. Visual categorization and the parietal cortex. Front. Integr. Neurosci. 6 (May), 1–6. https://doi.org/10.3389/fnint.2012.00018.

Freedman, D.J., Assad, J.A., 2006. Experience-dependent representation of visual categories in parietal cortex. Nature 443 (7107), 85–88. https://doi.org/10.1038/nature05078.

Freedman, David J., Assad, J.A., 2016. Neuronal mechanisms of visual categorization: an abstract view on decision making. Annu. Rev. Neurosci. 39 (1), 129–147. https://doi.org/10.1146/annurev-neuro-071714-033919.

Freedman, David J., Ibos, G., 2018. An integrative framework for sensory, motor, and cognitive functions of the posterior parietal cortex. Neuron 97 (6), 1219–1234. https://doi.org/10.1016/j.neuron.2018.01.044.

Freedman, David J., Riesenhuber, M., Poggio, T., Miller, E.K., 2001. Categorical representation of visual stimuli in the primate prefrontal cortex. Science (New York, N.Y.) 291 (5502), 312–316. https://doi.org/10.1126/science.291.5502.312.

Friston, K.J., Penny, W.D., Glaser, D.E., 2005. Conjunction revisited. Neuroimage 25 (3), 661–667.

Gardner, J.L., 2010. Is cortical vasculature functionally organized? Neuroimage 49 (3), 1953–1956.

Grefkes, C., Fink, G.R., 2005. The functional organization of the intraparietal sulcus in the macaque monkey. J. Anat. 207, 3–17. https://doi.org/10.1167/16.12.1302.
Handwerker, D.A., Ollinger, J.M., D'Esposito, M., 2004. Variation of BOLD hemodynamic responses across subjects and brain regions and their effects on statistical analyses. Neuroimage 21 (4), 1639–1651.
Haynes, JD, 2015. A primer on pattern-based approaches to fMRI: principles, pitfalls, and perspectives. Neuron. https://doi.org/10.1016/j.neuron.2015.05.025.
Jackson, J.B., Woolgar, A., 2018. Adaptive coding in the human brain: distinct object features are encoded by overlapping voxels in frontoparietal cortex. Cortex 108, 25–34. https://doi.org/10.1016/j.cortex.2018.07.006.
Jerde, T.A., Merriam, E.P., Riggall, A.C., Hedges, J.H., Curtis, C.E., 2012. Prioritized maps of space in human frontoparietal cortex. J. Neurosci. 32 (48), 17382–17390. https://doi.org/10.1523/jneurosci.3810-12.2012.
Kriegeskorte, N., Goebel, R., Bandettini, P., 2006. Information-based functional brain mapping. Proc. Natl. Acad. Sci. 103 (10), 3863–3868. https://doi.org/10.1073/pnas.0600244103.
Leathers, M.L., Olson, C.R., 2012. In monkeys making value-based decisions, LIP neurons encode cue salience and not action value. Science 338 (October), 132–135. https://doi.org/10.1126/science.1226405.
Lee, S.-H., Kravitz, D.J., Baker, C.I., 2013. Goal-dependent dissociation of visual and prefrontal cortices during working memory. Nat. Neurosci. 16 (8), 997–999. https://doi.org/10.1038/nn.3452.
Levine, S.M., Schwarzbach, J., 2017. Decoding of auditory and tactile perceptual decisions in parietal cortex. Neuroimage 162 (August), 297–305. https://doi.org/10.1016/j.neuroimage.2017.08.060.
Levine, S.M., Schwarzbach, J.V., 2018. Cross-decoding supramodal information in the human brain. Brain Struct. Funct. 223 (9), 4087–4098. https://doi.org/10.1007/s00429-018-1740-z.
Li, S., Ostwald, D., Giese, M., Kourtzi, Z., 2007. Flexible coding for categorical decisions in the human brain. J. Neurosci. 27 (45), 12321–12330. https://www.jneurosci.org/content/jneuro/27/45/12321.full.pdf.
Liu, T., Hou, Y., 2013. A hierarchy of attentional priority signals in human frontoparietal cortex. J. Neurosci. 33 (42), 16606–16616. https://doi.org/10.1523/jneurosci.1780-13.2013.
Logie, R.H., Cowan, N., 2015. Perspectives on Working Memory: Introduction to the Special Issue. Memory & Cognition. https://doi.org/10.3758/s13421-015-0510-x (March), 315–324.
Malone, P.S., Eberhardt, S.P., Wimmer, K., Sprouse, C., Klein, R., Glomb, K., et al., 2019. Neural mechanisms of vibrotactile categorization. Hum. Brain Mapp. 40 (10), 3078–3090. https://doi.org/10.1002/hbm.24581.
Muhammad, R., Wallis, J.D., Miller, E.K., 2006. A comparison of abstract rules in the prefrontal cortex, premotor cortex, inferior temporal cortex, and striatum. J. Cognit. Neurosci. 18 (6), 974–989. https://doi.org/10.1162/jocn.2006.18.6.974.
Nakayama, Y., Yamagata, T., Tanji, J., Hoshi, E., 2008. Transformation of a virtual action plan into a motor plan in the premotor cortex. J. Neurosci. 28 (41), 10287–10297. https://doi.org/10.1523/jneurosci.2372-08.2008.
Nichols, T., Brett, M., Andersson, J., Wager, T., Poline, J.B., 2005. Valid conjunction inference with the minimum statistic. Neuroimage 25 (3), 653–660.
Nieder, A., 2012. Supramodal numerosity selectivity of neurons in primate prefrontal and posterior parietal cortices. Proc. Natl. Acad. Sci. Unit. States Am. 109 (29), 11860–11865. https://doi.org/10.1073/pnas.1204580109.
Nieder, A., Diester, I., Tudusciuc, O., 2006. Temporal and spatial enumeration processes in the primate parietal cortex. Science 313 (September), 1431.
Nieder, Andreas, Miller, E.K., 2004. A parietol-frontal network for visual numerical information in the monkey. Proc. Natl. Acad. Sci. Unit. States Am. 101 (19), 7457–7462.
Oristaglio, J., Schneider, D.M., Balan, P.F., Gottlieb, J., 2006. Integration of visuospatial and effector information during symbolically cued limb movements in monkey lateral intraparietal area. J. Neurosci. 26 (32), 8310–8319. https://doi.org/10.1523/jneurosci.1779-06.2006.
Ostwald, D., Schneider, S., Bruckner, R., Horvath, L., 2019. Power, positive predictive value, and sample size calculations for random field theory-based fMRI inference. BioRxiv 613331. https://doi.org/10.1101/613331.
Polanía, R., Paulus, W., Nitsche, M.A., 2011. Noninvasively decoding the contents of visual working memory in the human prefrontal cortex with high-gamma oscillatory patterns. J. Cognit. Neurosci. 24, 304–314.
Postle, B.R., 2006. Working memory as an emergent property of the mind and brain. Neuroscience 139 (1), 23–38. https://doi.org/10.1016/j.neuroscience.2005.06.005.
Romo, R., Brody, C.D., Hernández, a, Lemus, L., 1999. Neuronal correlates of parametric working memory in the prefrontal cortex. Nature 399 (6735), 470–473. https://doi.org/10.1038/20939.
Rossi-Pool, R., Salinas, E., Zainos, A., Alvarez, M., Vergara, J., Parga, N., Romo, R., 2016. Emergence of an abstract categorical code enabling the discrimination of temporally structured tactile stimuli. Proc. Natl. Acad. Sci. Unit. States Am. https://doi.org/10.1073/pnas.1618196113, 201618196.
Rossi-Pool, R., Zainos, A., Alvarez, M., Zizumbo, J., Vergara, J., Romo, R., 2017. Decoding a decision process in the neuronal population of dorsal premotor cortex. Neuron 96 (6), 1432–1446. https://doi.org/10.1016/j.neuron.2017.11.023 e7.
Rossi-Pool, R., Zizumbo, J., Alvarez, M., Vergara, J., Zainos, A., Romo, R., 2019. Temporal signals underlying a cognitive process in the dorsal premotor cortex. Proc. Natl. Acad. Sci. Unit. States Am. 116 (15), 7523–7532. https://doi.org/10.1073/pnas.1820474116.
Sarma, A., Masse, N.Y., Wang, X.-J., Freedman, D.J., 2016. Task-specific versus generalized mnemonic representations in parietal and prefrontal cortices. Nat. Neurosci. 19 (1), 143–149. https://doi.org/10.1038/nn.4168.
Schmidt, T.T., Wu, Y., Blankenburg, F., 2017. Content-specific codes of parametric vibrotactile working memory in humans. J. Neurosci. 37 (40), 9771–9777. https://doi.org/10.1523/jneurosci.1167-17.2017.
Seger, C.A., Miller, E.K., 2010. Category learning in the brain. Annu. Rev. Neurosci. 33 (1), 203–219. https://doi.org/10.1146/annurev.neuro.051508.135546.
Senoussi, M., Berry, I., VanRullen, R., Reddy, L., 2016. Multivoxel object representations in adult human visual cortex are flexible: an associative learning study. J. Cognit. Neurosci. 28 (6), 852–868. https://doi.org/10.1162/jocn_a_00933.
Spitzer, B., Wacker, E., Blankenburg, F., 2010. Oscillatory correlates of vibrotactile frequency processing in human working memory. J. Neurosci. 30 (12), 4496–4502. https://doi.org/10.1523/JNEUROSCI.6041-09.2010.
Sprague, T.C., Ester, E.F., Serences, J.T., 2014. Reconstructions of information in visual spatial working memory degrade with memory load. Curr. Biol. 24 (18), 2174–2180. https://doi.org/10.1016/j.cub.2014.07.066.
Sprague, T.C., Ester, E.F., Serences, J.T., 2016. Restoring latent visual working memory representations in human cortex. Neuron 91 (3), 694–707. https://doi.org/10.1016/j.neuron.2016.07.006.
Sreenivasan, K.K., D'Esposito, M., 2019. The what, where and how of delay activity. Nat. Rev. Neurosci. 10–14. https://doi.org/10.1038/s41583-019-0176-7.
Stoet, G., Snyder, L.H., 2004. Single neurons in posterior parietal cortex of monkeys encode cognitive set. Neuron 42 (6), 1003–1012. https://doi.org/10.1016/j.neuron.2004.06.003.
Swaminathan, S.K., Freedman, D.J., 2012. Preferential encoding of visual categories in parietal cortex compared with prefrontal cortex. Nat. Neurosci. 15 (2), 315–320. https://doi.org/10.1038/nn.3016.
Tudusciuc, O., Nieder, A., 2007. Neuronal population coding of continuous and discrete quantity in the primate posterior parietal cortex. Proc. Natl. Acad. Sci. Unit. States Am. 104 (36), 14513–14518. https://doi.org/10.1073/pnas.0705495104.
Uluç, I., Schmidt, T.T., Wu, Y. Hao, Blankenburg, F., 2018. Content-specific codes of parametric auditory working memory in humans. Neuroimage 183, 254–262. https://doi.org/10.1016/j.neuroimage.2018.08.024.
Vallentin, D., Bongard, S., Nieder, A., 2012. Numerical rule coding in the prefrontal, premotor, and posterior parietal cortices of macaques. J. Neurosci. 32 (19), 6621–6630. https://doi.org/10.1523/jneurosci.5071-11.2012.
Wallis, J.D., Miller, E.K., 2003. From rule to response: neuronal processes in the premotor and prefrontal cortex. J. Neurophysiol. 90 (3), 1790–1806. https://doi.org/10.1152/jn.00086.2003.
Wen, T., Mitchell, D.J., Duncan, J., 2018. Response of the multiple-demand network during simple stimulus discriminations. Neuroimage 177 (March), 79–87. https://doi.org/10.1016/j.neuroimage.2018.05.019.
Wise, S.P., 1985. The primate premotor cortex: past, present, and preparatory. Annu. Rev. Neurosci. 8, 1–19.
Woolgar, A., Hampshire, A., Thompson, R., Duncan, J., 2011. Adaptive coding of task-relevant information in human frontoparietal cortex. J. Neurosci. 31 (41), 14592–14599. https://doi.org/10.1523/jneurosci.2616-11.2011.
Yamagata, T., Nakayama, Y., Tanji, J., Hoshi, E., 2012. Distinct information representation and processing for goal-directed behavior in the dorsolateral and ventrolateral prefrontal cortex and the dorsal premotor cortex. J. Neurosci. 32 (37), 12934–12949. https://doi.org/10.1523/jneurosci.2398-12.2012.
Yamagata, Tomoko, Nakayama, Y., Tanji, J., Hoshi, E., 2009. Processing of visual signals for direct specification of motor targets and for conceptual representation of action targets in the dorsal and ventral premotor cortex. J. Neurophysiol. 102 (6), 3280–3294. https://doi.org/10.1152/jn.00452.2009.
Zalesky, A., Cocchi, L., Fornito, A., Murray, M.M., Bullmore, E.D., 2012. Connectivity differences in brain networks. Neuroimage 60 (2), 1055–1062.
Zhong, L., Zhang, Y., Duan, C.A., Deng, J., Pan, J., Xu, N. Long, 2019. Causal contributions of parietal cortex to perceptual decision-making during stimulus categorization. Nat. Neurosci. 22 (6), 963–973. https://doi.org/10.1038/s41593-019-0383-6.
Zhou, Y., Freedman, D.J., 2019. Posterior parietal cortex plays a causal role in perceptual and categorical decisions. Science 2 (July), 1–5. https://doi.org/10.1007/978-1-4614-7320-6_310-1.